Journal of
Applied Remote Sensing

RemoteSensing.SPIEDigitalLibrary.org

Measurement of atmospheric oxygen using long-path supercontinuum absorption spectroscopy

David M. Brown
Andrea M. Brown
Perry S. Edwards
Zhiwen Liu
C. Russell Philbrick

SPIE.

Measurement of atmospheric oxygen using long-path supercontinuum absorption spectroscopy

David M. Brown,[a,b,*] Andrea M. Brown,[a,b] Perry S. Edwards,[a] Zhiwen Liu,[a] and C. Russell Philbrick[a,c]

[a]Pennsylvania State University, Department of Electrical Engineering, University Park, Pennsylvania 16802, United States

[b]Johns Hopkins University Applied Physics Laboratory, 11100 Johns Hopkins Road, Laurel, Maryland 20723, United States

[c]North Carolina State University, Departments of Physics and MEAS, Raleigh, North Carolina 27695-8202, United States

Abstract. The concentration of atmospheric oxygen is measured over a 540-m path using supercontinuum absorption spectroscopy. The absorption data compared favorably with MODTRAN™ 5 simulations of the spectra after adjusting for the differences of index of refraction of air and matching the instrument spectral resolution, as described by the effective slit width. Good agreement with the expected atmospheric oxygen concentration is obtained using a previously developed multiwavelength maximum likelihood estimation inversion algorithm. This study demonstrates the use of the SAS technique for measuring concentrations of chemical species with fine absorption structure on long-atmospheric paths. [DOI: 10.1117/1.JRS.8.083557]

Keywords: atmospheric species concentrations; supercontinuum laser; atmospheric differential absorption; differential absorption lidar; remote sensing.

Paper 14186 received Mar. 28, 2014; revised manuscript received Aug. 6, 2014; accepted for publication Aug. 11, 2014; published online Sep. 3, 2014.

1 Introduction

The supercontinuum source is a broadband spatially coherent photon emitter. We show that this source can be used to detect and characterize atmospheric constituents over a long path by measuring the spectra over a range of wavelengths. This source serves as an important alternative to frequency agile and tunable lasers, broadband incoherent sources, or the use of multiple single-wavelength lasers. Researchers have previously shown that the white light from ultrashort terawatt femtosecond pulses can be used to quantify the concentration of various atmospheric species using remotely generated plasma.[1,2] The same approach was also used to characterize aerosols along a path by monitoring the intensity variations of the scattering phase function for a range of backscattering angles.[3,4] Earlier approaches, often referred to as differential optical absorption spectroscopy (DOAS), employed lamps or lasers to make horizontal path absorption measurements.[5–9] Tomographic routines analogous to those developed through the work of Hashmonay and Yost[10] and Price[11] can then be employed to retrieve a range-resolved component for long-path absorption measurements.

Supercontinuum absorption spectroscopy (SAS) provides an important and useful alternative to classic DOAS for measuring atmospheric constituents along a predetermined path. The transmitter technology we use involves the coupling of subnanosecond pulses from a Q-switched Nd:YAG laser (JDSU, Milipitas, California NP-10620-100) into a photonic crystal fiber (Blaze Photonics, Bath, England SC-5.0-1040), thereby creating a broadband supercontinuum light source. This technique of supercontinuum generation was originally reported by Wadsworth

*Address all correspondence to: David M. Brown, E-mail: david.m.brown@jhuapl.edu

et al.,[12] and we have used it for a variety of studies in the laboratory and outdoor environment tests.[13,14] In fact, our prior work[13] describes the first time this technology was applied to outdoor measurements of atmospheric constituents. In that effort, SAS measurements of the water vapor absorption spectrum in the near-infrared (NIR) were measured and analyzed using a maximum likelihood estimation algorithm to quantify the concentration of water vapor over a several hundred meter outdoor path. Others have extended the original SAS approach to detect other atmospheric species in an indoor laboratory setting, such as CO_2.[15] Some groups have published the results of efforts where they examine laboratory mixtures of chemical species in gas cells.[16,17] The following describes our work to perform outdoor SAS measurements of atmospheric oxygen concentration along a longer 540-m free-space optical path.

2 Experimental Setup and Data Collection

Early versions of our SAS instrument demonstrated accurate measurements of water vapor over a 300-m path using only a few milliwatts of power.[13] The second-generation SAS system, which is described in the following paper, has increased signal-to-noise and therefore supports measurements along longer atmospheric paths. Furthermore, a high-resolution spectrograph on the receiver side permits measurements of species with fine absorption features at atmospheric pressure and temperatures. To demonstrate the operation of this instrument, a 540-m total outdoor folded path on a 135-m rooftop base path on the Penn State University campus between the Electrical Engineering East (EE East) building and the Dieke building was selected. A 30-cm square mirror was placed on the Dieke building and oriented nearly normal to the beam path to reflect the supercontinuum beam back to a retroreflector target on the rooftop of the EE East building. The retroreflector target used in this experiment is a gold-flashed corner cube with a 10 cm clear aperture that returns the beam over the 270-m path to a receiving telescope. The telescope receiver is a commercial-off-the-shelf Dobsonian telescope with a primary mirror diameter of 15 cm. The overall system architecture of the second-generation SAS system is also slightly different than that of prior versions. These changes in architecture include the relocation of the supercontinuum source and spectrograph detector to a basement laboratory. The transmitted and received lights are then transported via fiber optics to the free-space optical transceiver system located in the rooftop laboratory. Additional optical filtering in the system was required following this reconfiguration, and these important details are described in subsequent sections of this work.

In support of the second-generation SAS instrument design, we calculate the expected beam size for the 4-mm initial beam diameter, as a function of range for a 760-nm center wavelength. The result is shown in Fig. 1. The calculation assumes that the supercontinuum light being transmitted to the atmospheric path has a good beam profile, so we set the beam quality, M^2, equal to one for this example. Turbulence free and extremely heavy turbulence conditions, $C_n^2 = 10^{-19}$ m$^{-2/3}$ and $C_n^2 = 10^{-12}$ m$^{-2/3}$, respectively, are included in the calculations;

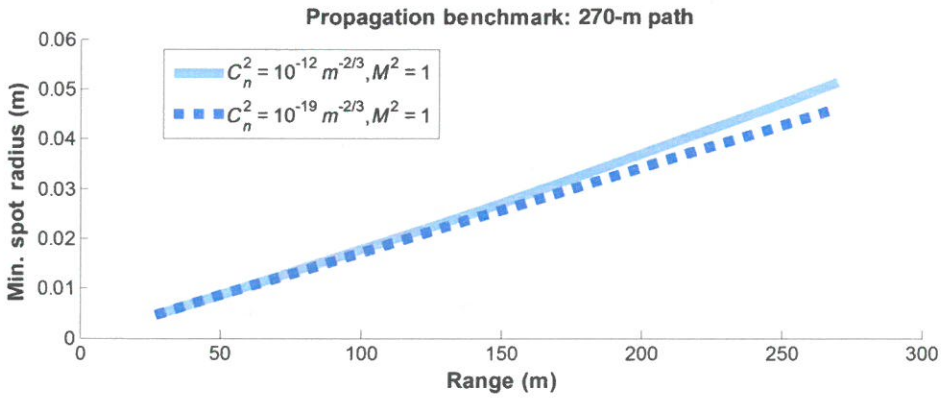

Fig. 1 Calculations of beam-spread size are plotted as a function of range for minimum and maximum turbulence conditions.

however, the figure shows that the turbulence does not strongly affect the beam size at the extent of the proposed propagation distance. These simple calculations confirm that a transmitted beam with an approximate diameter of 4 mm at the source is well matched to the retroreflector target at a range of 270 m. This is important to ensure that the received signal is strong and not significantly impacted by atmospheric turbulence which can change over time.

The desired transmitted beam size is created by collimating the supercontinuum light emanating from the basement-to-roof single-mode transport fiber using a 10× microscope objective with an 18-mm focal length. We are unable to perfectly collimate the light at all wavelengths because we are using a refractive collimating optic, so we adjust this to optimize the collimation for the 600- to 800-nm wavelength range.

The second-generation SAS system uses a Princeton Instruments (Trenton, New Jersey) Acton Spectrometer (SP-2500i and SPEC-10 liquid-nitrogen cooled CCD), which is typically configured for a 0.03-nm (0.5 cm^{-1}) resolution at 760 nm to analyze the return signal. As mentioned previously, the spectrometer and supercontinuum source are located in a basement laboratory and fiber optic cables are used to transfer the signals to and from the rooftop laboratory, where the transmitter/receiver are located, as depicted in Fig. 2. With this configuration, we are able to reduce the environmental effects on the transmitted signal intensity, which were routinely observed in signals measured by the first-generation SAS system.[13] Prior to this relocation, we had typically experienced up to 50% optical power variations during tens of minutes to an hour of operation due to thermal effects when the supercontinuum source itself was located in the rooftop laboratory. This measurement was performed with a broadband power meter placed at the output of the 18-m Blaze Photonics's photonic crystal fiber used to generate the supercontinuum light source. We attribute those variations to temperature changes that caused expansion and contraction of the aluminum-mounting hardware, which misaligned the microchip laser coupling optics used to generate the supercontinuum spectrum. When the supercontinuum source was relocated to the basement laboratory, power variations were vastly reduced and were insignificant over the period of time for a measurement.

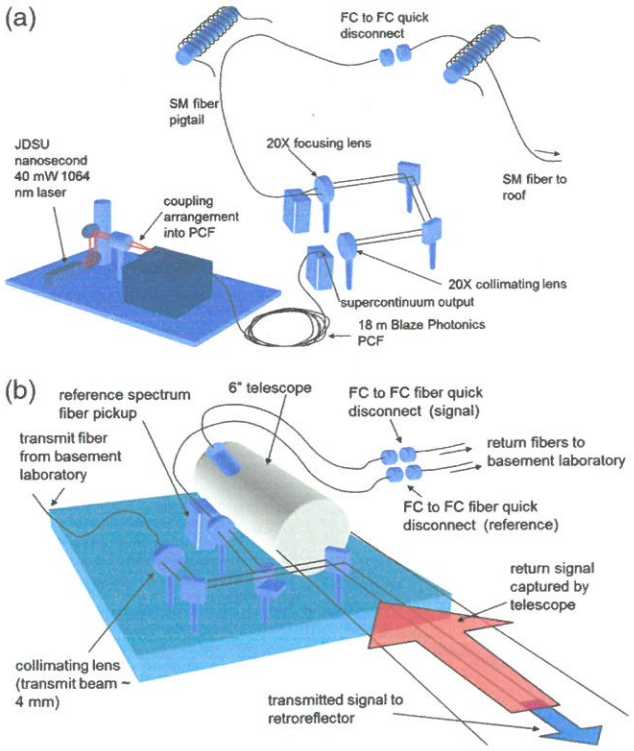

Fig. 2 Second-generation supercontinuum absorption spectroscopy (SAS) experimental setup used for collecting data reported here: (a) the supercontinuum source in the basement laboratory and (b) the transmitter and receiver arrangements in the rooftop laboratory.

After relocating the laser source to the basement laboratory to minimize the temperature effects, a lesser variation in the spectral nature of the supercontinuum source was realized. After several empirical studies, we established that these remaining variations were associated with two sources. The cause and mitigation approach for both are described as follows.

First, we noted that the baseline of the supercontinuum source spectra within our wavelength range of interest for oxygen absorption spectra changed over the course of hours. A MODTRAN™ 5 (Ref. 18) calculation of atmospheric transmission between 755 and 775 nm for a mid-latitude winter atmosphere with 50-km visibility is shown in Fig. 3(a) for comparison. An example of the baseline change observed in this 20-nm band is depicted in the overall slope changes of the spectra from being positive in Fig. 3(b) to negative in Fig. 3(c). The cause of these variations was determined to be a slight change in coupling efficiency of the 20× microscope objective lens and single mode-fiber combination used to optically couple and transport the supercontinuum source spectra to the rooftop laboratory [see Fig. 2(a)]. A free-space reference path up to the roof laboratory and back to the basement lab was used to normalize the baseline of the supercontinuum beam transmitted through the atmospheric measurement path.

The focusing of the light into the signal and reference path fibers from the rooftop to the basement utilized low-power singlet lenses to increase the size of the focal spot on the tip of the fiber face. By collecting the reference and signal spectra in this way, we were able to minimize the impact of alignment errors and aberrations on the system. The temperature-stabilized

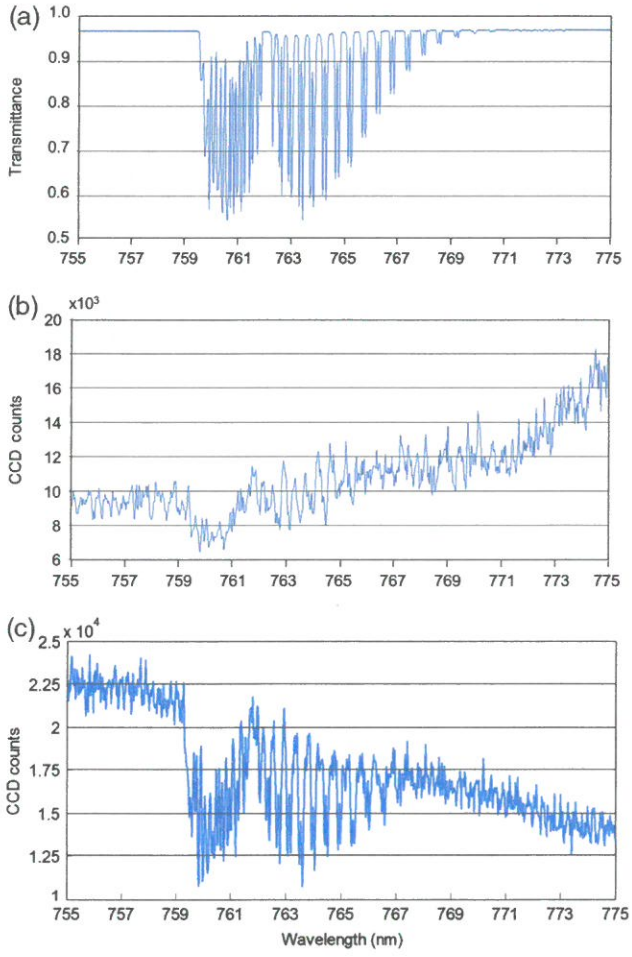

Fig. 3 (a) Calculated MODTRAN™ 5 reference spectrum for oxygen absorption on a 540-m path, (b) initial unfiltered SAS measurements of oxygen, and (c) oxygen absorption signal measured on 540-m path after modal filter use to reduce the spectral noise of the fiber-delivered supercontinuum.

supercontinuum source combined with this configuration of the signal and reference collection optics reduced the temporal drift in the spectral baseline and the overall power of the signal and reference channels to indiscernible levels over the period of the measurement. The optical throughput was greatly reduced by employing this approach; however, this was offset by the high sensitivity of the spectroscopic detection system located in the basement laboratory.

The second source of variation in our collected experimental long-path spectra was due to the launching of high-order modes in the 20-m long transport fibers to and from the basement laboratory. This occurs because the transport fibers are designed to be single mode at the telecommunication wavelengths; hence, they are still slightly multimode at the visible wavelengths of interest in our study. The multimode nature of the fiber in our wavelength range of interest tends to create a wavelength-dependent modulation in the fiber loss term. This spectrally varying modulation is best observed by again reviewing Fig. 3(b). We find that while we are able to discern the oxygen absorption structure in the experimental data of Fig. 3(b), its signature is superimposed on a spectral noise background, which is due to the variations in multimode propagation of the light down the fiber. These background variations in the supercontinuum spectra observed are on the order of 0.1 to 0.5 nm, which is the same scale size as features in the absorption spectrum of oxygen; therefore, it is difficult to make a determination of the oxygen concentration when using the raw spectral data. Modal filters, which mitigate these effects, were subsequently added to the setup.

Other researchers have developed modal filters which allow the higher-order modes to leak from the core-cladding interface of the optical fiber.[19] Similar to those published techniques, we created filters by coiling the jacketed fibers around five different radii mandrels ranging from 5 to 20 mm. The coil diameter and sequence most appropriate are empirically determined and found to be a configuration consisting of 720 deg (two full rotations) coiled around 20-, 15-, 10-, 7.5-, and 5-mm rods, respectively. These sequences of rotations are inserted after the supercontinuum light is coupled into the single-mode fiber pigtail and again following the FC/FC butt-coupled connector (see Fig. 2). This quick disconnect coupling enables the user to quickly examine and maximize the power being transmitted to the roof, but it also relaunches a few higher-order modes into the fiber. These modes are subsequently removed by inserting a second modal filter, identical to the first. The same matched modal filter approach was used for the signal and reference path fibers on the return side of the instrument. The array of small radii coils is highly lossy; however, the configuration inhibits the propagation of nearly all high-order modes in the fiber links. As time slowly changes the coupling efficiency of the light into the fiber, the launched higher-order modes also will change; however, they are then filtered out by the modal filters. To summarize, the technique described results in a stable spectral profile of NIR supercontinuum light transmitted to and received by the retroreflector target 270-m downrange, and an example of this result is shown in Fig. 3(c). An important topic of future work will be the acquisition of a dataset aimed at establishing the types and magnitudes of all errors and uncertainties with and without different filtering and averaging schemes. A number of relevant examples pertaining to

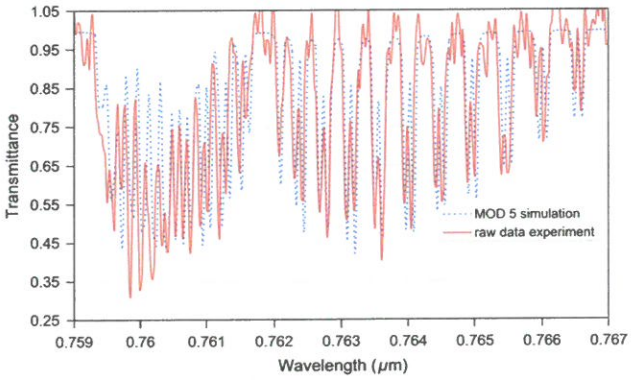

Fig. 4 SAS oxygen absorption measurement on 540-m path is compared with MODTRAN™ 5 calculation using the refractive index of air calculated from Eq. (1).

a different but related field of diode laser absorption spectroscopy can be found by reviewing the work of Werle et al.[20]

3 Data Analysis

An example high-resolution, normalized, and mode-filtered experimental optical spectra is found in Fig. 4 as the solid line. In the same figure, this measured absorption structure of molecular oxygen is accompanied with a model simulation (dashed line) for an equivalent path length and spectral slit width. Note that this experimental result is a single-spectral acquisition that has not been spectrally or temporally averaged. The calculated transmission spectra were generated using the high-resolution capability in MODTRAN™ 5 (0.1 cm^{-1}, 0.006 nm at 760 nm) to simulate the horizontal path through the atmosphere. A 0.2 to 0.3 nm offset between simulation and experimental results was initially observed when comparing the SAS experimental data with the MODTRAN™ 5 simulated spectra. Prior to the current work, the 1-cm^{-1} resolution available in the earlier MODTRAN™ 4 version was used for comparison with atmospheric water vapor absorption measurements at lower resolution.[13] The lower-resolution MODTRAN calculation had previously masked the difference caused by using the vacuum refractive index.[21] Converting the MODTRAN™ 5 outputs to the air value using Eq. (1) (units of λ are nanometers)[22,23] resulted in reasonable agreement between the normalized SAS return spectra and the MODTRAN™ 5 simulated spectra of oxygen absorption, as shown in Fig. 4.

$$\lambda_{\text{air}} = \frac{\lambda_{\text{vac}}}{1.0 + 2.735182 \times 10^{-4} + \frac{13.14182}{\lambda_{\text{vac}}^2} + \frac{2.76249 \times 10^5}{\lambda_{\text{vac}}^4}}. \tag{1}$$

The collected SAS data are then processed with a multiwavelength maximum likelihood estimation (MLE) algorithm, which is fully described in earlier reports.[13,21] In the case of the present work, the MLE algorithm provides a way to experimentally determine the concentration of oxygen along the measurement path. This algorithmic approach was originally developed by following the work of Warren[24] and was later expanded by Yin and Wang.[25] An 8-nm spectral region that bounds the oxygen absorption structure located from 759 to 767 nm is selected for the study, and is sampled at various wavelength locations prior to serving as an input to the MLE algorithm. Twenty spectral acquisitions of this region of interest served as the input data matrix for the MLE algorithm. Each of the spectral acquisitions was obtained over a 10-s time period during the first 10 s of every minute for 20 min. The experimental data were then filtered with a raised cosine filter with a 0.4-nm full-width half-maximum before inverting the measurement. This spectral smoothing was performed prior to algorithmic estimation of oxygen concentration to reduce the noise present in the raw normalized spectra that would

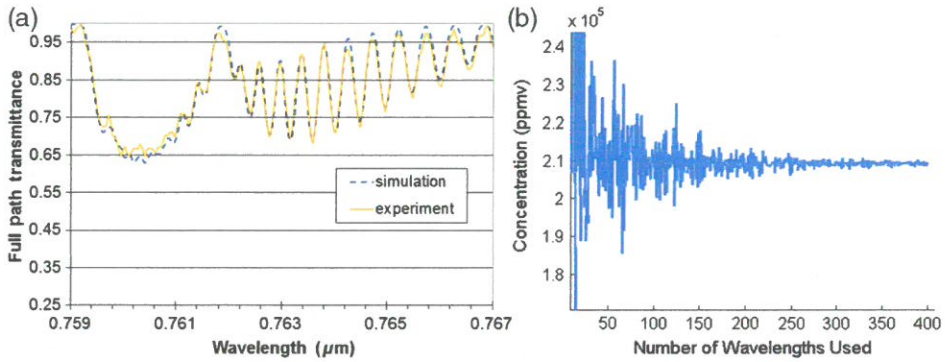

Fig. 5 Oxygen concentration measurements on a 540-m path: (a) spectrally smoothed SAS data compared with a MODTRAN™ 5 calculation, and (b) multiwavelength maximum likelihood estimation (MLE) algorithm showing the convergence of the algorithm for calculation of atmospheric oxygen concentration.

slow and sometimes inhibit the MLE algorithm from producing a clean convergence. An example of the spectrally averaged, normalized measurement compared with a MODTRAN™ 5 simulation of the spectral region is shown in Fig. 5(a).

The MLE results are shown as a function of the number of linearly spaced wavelengths used for different executions of the inversion algorithm [see Fig. 5(b)]. The figure reveals that as more wavelengths are used, the mean experimental atmospheric oxygen concentration converges to 209,180 ppm. This measured concentration can then be compared with the standard atmospheric value of 20.946%,[26] or 209,460 ppm. Here, we note that our analysis has incorporated the use of hundreds of wavelength pairs and all the spectral acquisitions obtained over the 20-min measurement period; therefore, it is a time-averaged result. The standard deviation in the experimental result over this time period depends on the number and wavelength location of the spectral data points extracted from the experimentally measured spectrum. As a point of comparison, the standard deviation in the algorithmic result, if 350 to 400 wavelengths are used in the analysis, is 460 ppm. A more appropriate comparison, however, is to examine the 280-ppm difference between the measured mean concentration of 209,180 ppm to the atmospheric average concentration of 209,460 ppm. The reason for the difference from the standard atmospheric concentration of oxygen is due to a combination of effects. A primary error source is the uncertainty in the path length, which was measured with a low-resolution ($\pm$0.5 m) laser range finder. This half-meter path length error can introduce ~193 ppm of uncertainty into the measured experimental atmospheric oxygen concentration. An additional error source could be due to variations in temperature, pressure, water vapor, or other species present along the path. For example, in the case of temperature alone, using the ideal gas law, we calculate that a 1°C change in temperature changes the oxygen concentration in air by 0.07%, or 146 ppm. Single and even multiple degree fluctuations in temperature along such a path are certainly possible given the urban environment where the experiment was performed. In the case of water vapor or other atmospheric species, these materials will displace the oxygen molecules along the path, thereby varying the path-averaged result. Future measurements will include improved path length measurements, precise monitoring of environmental variables, and more sophisticated data analysis techniques, such as the spectral unmixing of supercontinuum spectra.[27]

4 Summary

This report is intended to underscore several topics learned while conducting this research. First, SAS technology provides a useful alternative method to DOAS, differential absorption and scattering (DAS), and differential absorption lidar (DIAL) techniques to enable long-path spectroscopic measurements while using only milliwatts of transmitted power. Second, the SAS transmitter and receiver can be fiber optically coupled to a transceiver located more than 20 m away, thereby easing the logistical implementation of such a measurement system. This system configuration would be attractive for a variety of applications, as the laser and detector system can be located in a single location and fibers can be used to route to a variety of optical transceiver locations. Specifically, such an approach would be ideal for performing air-quality measurements over numerous atmospheric paths in an urban environment. Third, a multiwavelength MLE estimation algorithm developed for DIAL has been slightly modified for use with SAS data to determine atmospheric species concentrations. A large number of wavelengths can be used in the inversion process because the supercontinuum source spans many absorption lines of a chemical species. Additionally, the wavelength ratios used for concentration analysis are simultaneously acquired by the instrument given the broadband source and detector combination.

In summary, the SAS technique provides accurate long-path measurements of optical absorption simultaneously measured at multiple on-line and off-line wavelengths. We have demonstrated in this work that the approach can be used to characterize atmospheric species by using their associated fine absorption spectra. Future efforts, which make use of higher power supercontinuum laser sources, should enable range-resolved returns by scattering from the molecular and aerosol backgrounds along the path to provide simultaneous profiles of many species concentrations.

References

1. P. Rairoux et al., "Remote sensing of the atmosphere using ultrashort laser pulses," *Appl. Phys. B* **71**(4), 573–580 (2000).
2. M. Rodriguez et al., "Femtosecond LIDAR: new perspectives of atmospheric remote sensing," *Proc. SPIE* **5149**, 135–143 (2003).
3. R. Bourayou et al., "White-light filaments for multiparameter analysis of cloud microphysics," *J. Opt. Soc. Am. B* **22**(2), 369 (2005).
4. M. C. Galvez et al., "Three-wavelength backscatter measurement of clouds and aerosols using a white light lidar system," *Jpn. J. Appl. Phys.* **41**(3A), L284–L286 (2002).
5. R. R. Patty et al., "CO_2 laser absorption coefficients for determining ambient levels of O_3, NH_3, and C_2H_4," *Appl. Opt.* **13**(12), 2850–2854 (1974).
6. W. A. McClenny and G. M. Russwurm, "Laser-based, long path monitoring of ambient gases—analysis of two systems," *Atmos. Environ.* **12**(6–7), 1443–1453 (1978).
7. U. Platt, D. Pemer, and H. W. Patz, "Simultaneous measurement of atmospheric CH_2O, O_3, and NO_2 by differential optical absorption," *J. Geophys. Res.* **84**(C10), 6329–6335 (1979).
8. U. Platt and D. Perner, "Measurements of atmospheric trace gases by long path differential UV/visible absorption spectroscopy," *Springer Ser. Opt. Sci.* **39**, 97–105 (1983).
9. U. Platt and J. Stutz, *Differential Optical Absorption Spectroscopy: Principles and Applications*, Springer-Verlag, Berlin (2008).
10. R. A. Hashmonay and M. G. Yost, "Innovative approach for estimating gaseous fugitive fluxes using computed tomography and remote optical sensing techniques," *J. Air Waste Manage. Assoc.* **49**(8), 966–972 (1999).
11. P. N. Price, "Pollutant tomography using integrated concentration data from non-intersecting optical paths," *Atmos. Environ.* **33**(2), 275–280 (1999).
12. W. Wadsworth et al., "Supercontinuum and four-wave mixing with Q-switched pulses in endlessly single-mode photonic crystal fibers," *Opt. Express* **12**(2), 299–309 (2004).
13. D. M. Brown et al., "Long-path supercontinuum absorption spectroscopy for measurement of atmospheric constituents," *Opt. Express* **16**(12), 8457–8471 (2008).
14. P. S. Edwards et al., "Supercontinuum laser sensing of atmospheric constituents," *Proc. SPIE* **7323**, 73230S (2009).
15. T. Somekawa et al., "Differential optical absorption spectroscopy measurement of CO_2 using a nanosecond white light continuum," *Opt. Lett.* **36**(24), 4782–4784 (2011).
16. A. Dobroc and N. Cézard, "Performance assessment, and signal processing for range integrated concentration measurement of gas species using supercontinuum absorption spectroscopy," *Appl. Opt.* **51**(35), 8470–8480 (2012).
17. N. Cézard et al., "Supercontinuum laser absorption spectroscopy in the mid-infrared range for identification and concentration estimation of a multi-component atmospheric gas mixture," *Proc. SPIE* **8182**, 81820V (2011).
18. A. Berk et al., "MODTRAN5: a reformulated atmospheric band model with auxiliary species and practical multiple scattering options," *Proc. SPIE* **5655**, 88–95 (2005).
19. Y. Koyamada and K. Yamashita, "Launching condition dependence of graded-index multimode fiber loss, and bandwidth," *J. Lightwave Technol.* **6**(12), 1866–1871 (1988).
20. P. Werle et al., "Signal processing and calibration procedures for in situ diode-laser absorption spectroscopy," *Spectrochim. Acta A* **60**(8–9), 1685–1705 (2004).
21. D. M. Brown, Z. Liu, and C. R. Philbrick, "Supercontinuum lidar applications for measurements of atmospheric constituents," *Proc. SPIE* **6950**, 69500B (2008).
22. G. Bonsch and E. Potulski, "Measurement of the refractive index of air and comparison with modified Edlen's formula," *Metrologia* **35**(2), 133–139 (1998).
23. B. Edlen, "The refractive index of air," *Metrologia* **2**(2), 71–80 (1966).
24. R. E. Warren, "Optimum detection of multiple vapor materials with frequency agile lidar," *Appl. Opt.* **35**(21), 4180–4193 (1996).
25. S. Yin and W. Wang, "Novel algorithm for simultaneously detecting multiple vapor materials with multiple-wavelength differential absorption lidar," *Chin. Opt. Lett.* **4**, 360–362 (2006).

26. COESA, *U.S. Standard Atmosphere, 1976*, U.S. Government Printing Office, Washington, DC (1976).
27. J. Fade, S. Lefebvre, and N. Cézard, "Minimum description length approach for unmixing of multiple interfering gas species," *Opt. Express* **19**(15), 13863–13872 (2011).

David M. Brown received his PhD degree in electrical engineering from the Pennsylvania State University in 2008 and has nearly 10 years of experience in applied spectroscopy and remote sensing. He is a recognized expert in electro-optical systems and related fields, such as LIDAR and FTIR, investigations of atmospheric optical propagation for a variety of laser types, wave propagation modeling, turbulence, applied spectroscopy, atmospheric characterization, and standoff optical remote sensing. He routinely serves as a technical mentor and has published numerous technical reports, scientific papers, and journal articles.

Andrea M. Brown received her PhD degree in electrical engineering from the Pennsylvania State University in 2010 and has a strong academic background in electromagnetic theory. She has supported a wide variety of tasks that pertain to material characterization through optical scattering, including BRDF measurement and analysis and aerosol characterization. Her general theoretical work includes the use of MODTRAN™, Mie scattering, T-matrix, or various other types of programs or approximations to calculate the scattering or absorption cross-sections of particles of various shapes, sizes, and materials.

Perry S. Edwards received his PhD degree in electrical engineering from the Pennsylvania State University in 2013. As a student, he was a Diefenderfer fellowship recipient, awarded for scholarly achievement and to innovative, entrepreneurial-oriented engineering graduate students. He is currently the CEO and cofounder of Atoptix, LLC, which is a leading developer of miniature optical spectroscopy and sensor systems. He also has considerable expertise and has worked on numerous projects in the fields of optical remote sensing, nonlinear optics, and ultrafast laser systems. He is a member of SPIE and IEEE.

Zhiwen Liu is an associate professor of electrical engineering at the Pennsylvania State University. He received his PhD degree in electrical engineering from the California Institute of Technology in 2002. After staying at Caltech for a year as a postdoctoral researcher, he joined Penn State in 2003. His current research interest includes optical imaging and spectroscopy, ultrafast nonlinear optics, and nanophotonics.

C. Russell Philbrick retired from the AF Geophysics Laboratory in 1988 and from the Penn State University Department of Electrical Engineering in 2009 (emeritus professor); he returned to his alma mater, North Carolina State University, where he is a faculty member in the Physics and MEAS Departments. He enjoyed teaching during the past 25 years and continues research in optics, atmosphere and space physics, and encouraging graduate students and STEM teachers, while entering retirement years.